



Recent *Vibrio cholerae* O1 Epidemic Strains Are Unable To Replicate CTX Φ Prophage Genome

Kaoru Ochi,^a Tamaki Mizuno,^b Prosenjit Samanta,^c Asish K. Mukhopadhyay,^c Shin-ichi Miyoshi,^b  Daisuke Imamura^a

^aDepartment of Frontier Bioscience, Hosei University, Koganei, Tokyo, Japan

^bGraduate School of Medicine, Dentistry and Pharmaceutical Sciences, Okayama University, Okayama, Japan

^cDivision of Bacteriology, National Institute of Cholera and Enteric Diseases, Kolkata, India

ABSTRACT Cholera, an acute diarrheal disease, is caused by pathogenic strains of *Vibrio cholerae* generated by the lysogenization of the filamentous cholera toxin phage CTX Φ . Although CTX Φ phage in the classical biotype are usually integrated solitarily or with a truncated copy, those in El Tor biotypes are generally found in tandem and/or with related genetic elements. Due to this structural difference in the CTX Φ prophage array, the prophage in the classical biotype strains does not yield extrachromosomal CTX Φ DNA and does not produce virions, whereas the El Tor biotype strains can replicate the CTX Φ genome and secrete infectious CTX Φ phage particles. However, information on the CTX Φ prophage array structure of pathogenic *V. cholerae* is limited. Therefore, we investigated the complete genomic sequences of five clinical *V. cholerae* isolates obtained in Kolkata (India) during 2007 to 2011. The analysis revealed that recent isolates possessed an altered CTX Φ prophage array of the prototype El Tor strain. These strains were defective in replicating the CTX Φ genome. All recent isolates possessed identical *rstA* and intergenic sequence 1 (Ig-1) sequences and comparable *rstA* expression in the prototype El Tor strain, suggesting that the altered CTX Φ array was responsible for the defective replication of the prophage. Therefore, CTX Φ structures available in the database and literatures can be classified as replicative and nonreplicative. Furthermore, *V. cholerae* epidemic strains became capable of producing CTX Φ phage particles since the 1970s. However, *V. cholerae* epidemic strains again lost the capacity for CTX Φ production around the year 2010, suggesting that a significant change in the dissemination pattern of the current cholera pandemic occurred.

IMPORTANCE Cholera is an acute diarrheal disease caused by pathogenic strains of *V. cholerae* generated by lysogenization of the filamentous cholera toxin phage CTX Φ . The analysis revealed that recent isolates possessed altered CTX Φ prophage array of prototype El Tor strain and were defective in replicating the CTX Φ genome. Classification of CTX Φ structures in isolated years suggested that *V. cholerae* epidemic strains became capable of producing CTX Φ phage particles since the 1970s. However, *V. cholerae* epidemic strains again lost the capacity for CTX Φ production around the year 2010, suggesting that a critical change had occurred in the dissemination pattern of the current cholera pandemic.

KEYWORDS *Vibrio cholerae*, cholera, prophage

Cholera is an acute diarrheal disease and remains a major threat to health, particularly in developing countries (1, 2). It is caused by infection with toxigenic *Vibrio cholerae* strains (3). Although over 200 serogroups of *V. cholerae* have been identified, 2 serogroups (O1 and O139) are responsible for cholera epidemic and pandemic (4, 5). The serogroup O1 can be further classified into 2 biotypes (classical and El Tor). Toxigenic *V. cholerae* strains are generated by the infection and lysogenization of a

Citation Ochi K, Mizuno T, Samanta P, Mukhopadhyay AK, Miyoshi S-I, Imamura D. 2021. Recent *Vibrio cholerae* O1 epidemic strains are unable to replicate CTX Φ prophage genome. *mSphere* 6:e00337-21. <https://doi.org/10.1128/mSphere.00337-21>.

Editor Craig D. Ellermeier, University of Iowa

Copyright © 2021 Ochi et al. This is an open-access article distributed under the terms of the [Creative Commons Attribution 4.0 International license](https://creativecommons.org/licenses/by/4.0/).

Address correspondence to Daisuke Imamura, daisuke.imamura.58@hosei.ac.jp.

Received 7 April 2021

Accepted 25 May 2021

Published 9 June 2021

filamentous phage, CTX Φ (6). The genome of CTX Φ prophage contains *ctxAB*, which encodes cholera toxin, which is the primary virulence factor of cholera responsible for severe and watery diarrhea. Since 1817, seven pandemics of cholera have been recorded. The sixth and, presumably, the earlier pandemics emerged from the Gangetic delta and were caused by the classical biotype of *V. cholerae*, whereas the current ongoing seventh pandemic has been attributed to the El Tor biotype (5). The *V. cholerae* El Tor biotype has shown remarkable changes over the years of the seventh pandemic. A new pathogenic variant that possesses the classical type *ctxB* (*ctxB1*) with an El Tor type genomic backbone has emerged (7–10). More recently, the novel *ctxB* variant (*ctxB7*) has been found in Haiti and other countries (11, 12). Ghosh et al. demonstrated that the Haitian variant strain has evolved because of sequential events on the Indian subcontinent with some cryptic modification in the genome (13). Moreover, it has also been reported that the seventh pandemic strain first appeared in the Gangetic delta and recurrently spread from this area to the rest of the world, in at least three waves (14). Therefore, the Gangetic delta is considered the epicenter for all cholera pandemics according to the historical records. We recently isolated and characterized *V. cholerae* strains from patients suffering from cholera who were residing in Kolkata, India, which is a representative area of the Gangetic delta, between 2007 and 2014 (15). The analysis revealed that the cholera epidemics were caused by distinct *V. cholerae* O1 strains and that the predominant strains have undergone a shift in recent years.

Studies have indicated that the biotypes of pathogenic *V. cholerae* strains have generally been recognized based on the genotypes of pathogenic genes, including *ctxB* and/or phylogeny of the genomic backbone (14, 15). In addition to this analysis, diverse CTX Φ prophage arrays have also been found within strains isolated from epidemics (16). Classical strains usually possess a single CTX Φ genome or a CTX Φ genome with truncated copy on the larger chromosome and also have an additional single CTX Φ genome on the smaller chromosome (17). In two classical biotype strains (O395 and 569B), a truncated CTX Φ comprising *rstR*, *rstA*, and *rstB* and a partial *cep* followed by an intact CTX Φ genome in the larger chromosome (Fig. 1, top) and another CTX Φ prophage in the smaller chromosome are integrated (18). Although CTX Φ prophage genomes of these strains contain intact gene sets, CTX Φ is unable to replicate its genome due to the prophage array structure. The CTX Φ prophage genome in the El Tor biotype strains was usually found in tandem and/or with a related genetic element known as RS1 in the larger chromosome (16, 19). RS1 contains *rstC* and the following genes in CTX Φ phage: *rstR*, *rstA*, and *rstB* (Fig. 1A). CTX Φ prophage DNA is replicated by a rolling-circle mechanism that requires *rstA* (20). RstA nicks the plus strand DNA of the CTX Φ prophage genome at intergenic sequence 1 (I_g-1), which is located adjacent to *rstR* (Fig. 1B). The host replication machinery synthesizes a new plus strand, while displacing the old plus strand (Fig. 1C). Moreover, RstA also nicks the I_g-1 of the adjacent CTX Φ prophage or RS1 downstream of the CTX Φ prophage genome in the El Tor biotype, which releases a closed circular ssDNA (Fig. 1D, Moyer 2001). Thus, I_g-1 both upstream and downstream of the CTX Φ prophage genome (i.e., the presence of tandem elements, the presence of either of the two prophages, or the presence of a prophage followed by an RS1) is necessary for the replication of the CTX Φ genome. As a consequence, CTX Φ phage in the classical biotype strains does not yield extrachromosomal CTX Φ DNA and thus does not produce virions, whereas El Tor biotype strains can secrete infectious CTX Φ particles (17). These observations indicate that the transmission of CTX Φ genome from toxigenic *V. cholerae* to other strains during the sixth and earlier pandemics was not caused by the phage infection. It was restricted to natural competence or other indirect horizontal transfer of *V. cholerae*. In contrast, during the seventh pandemic, CTX Φ phage particles were produced from toxigenic *V. cholerae* and probably generated new toxigenic strains, spreading the infection in the environment. Hence, the dissemination and continuation patterns of cholera pandemics are dissimilar.

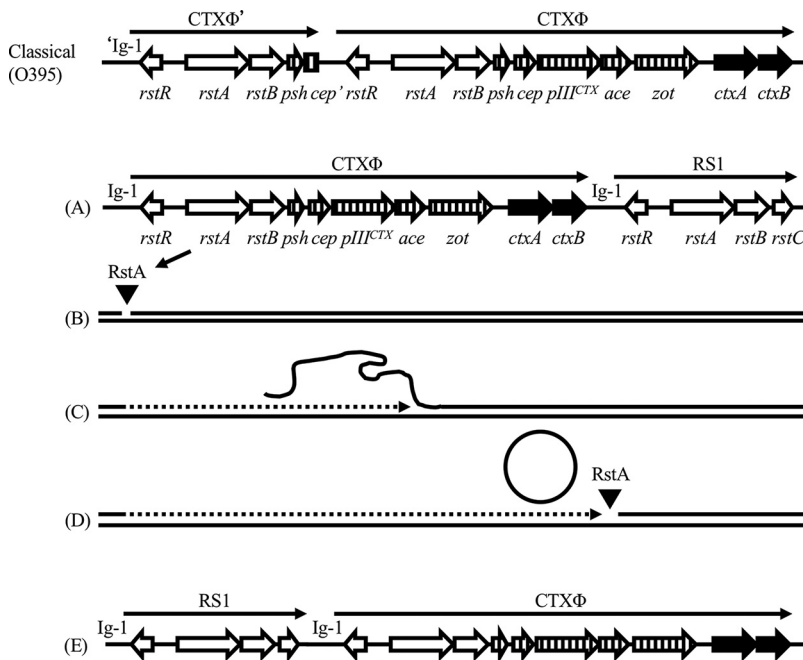


FIG 1 Model for the rolling-circle replication of the CTX Φ prophage genome. Genes in the CTX Φ prophage and its array in the classical biotype O395 and El Tor biotype N16961 are shown (top and panel A). Open arrows indicate the genes necessary for DNA replication and the integration of the phage. Striped arrows indicate the genes required for phage packaging and secretion (21). Solid arrows indicate the genes responsible for encoding the cholera toxin. *Ig-1* was located adjacent to *rstR* in CTX Φ and RS1, and the CTX Φ prophage genome was located between the two *Ig-1* sequences in the prototype El Tor biotype strain (A). *RstA* nicked *Ig-1* in the plus-strand DNA of CTX Φ (B). Host replication machinery synthesized a new plus strand while displacing the old plus strand (C). *RstA* nicked *Ig-1* at the downstream end of the CTX Φ prophage genome, resulting in a closed circular single-strand DNA (D). RS1 in recent isolates used in this study was located at the upstream end of the CTX Φ genome, compared with the prototype El Tor the biotype strains (E). This type of CTX Φ prophage lacked the *Ig-1* at the downstream end of the CTX Φ genome.

Recently we reported that two distinct lineages of pathogenic *V. cholerae* strains were concurrently prevalent between 2007 and 2009, while one lineage became predominant in 2010 and later in Kolkata, India (15). These investigations were performed by phylogenetic analyses, based on the single nucleotide polymorphisms of core genomic sequences, using short reads obtained with an Illumina next-generation sequencer. However, these analyses do not provide insights with respect to the copy number and array of repeated genomic sequences, which play important roles in the virulence of *V. cholerae* (21). To investigate the variations in the chromosomal structures of *V. cholerae* epidemic strains, including copy numbers and the arrangement of repeated sequences, we developed complete genomic sequences of five representative *V. cholerae* strains isolated from Kolkata, India, in this study. The analysis demonstrated that the recent epidemic strains of *V. cholerae* El Tor biotype possess both intact CTX Φ prophage and RS1, although in the altered array of prototype El Tor strains. The strains with an altered CTX Φ array were incapable of replicating the CTX Φ genome, suggesting that a critical change may have occurred in the dissemination and continuation route of the current cholera pandemic.

RESULTS

Structural variations in the genomes of recent *V. cholerae* epidemic strains. It was reported that two distinct lineages (1 and 2) of pathogenic *V. cholerae* strains were concurrently prevalent between 2007 and 2009, while lineage 2, sublineage III, appeared in 2010, followed by the predominance of lineage 2, sublineage IV, in 2011 and later in Kolkata, India (15). Two isolates, IDH-00113 (referred to here as strain 13) and IDH-02387

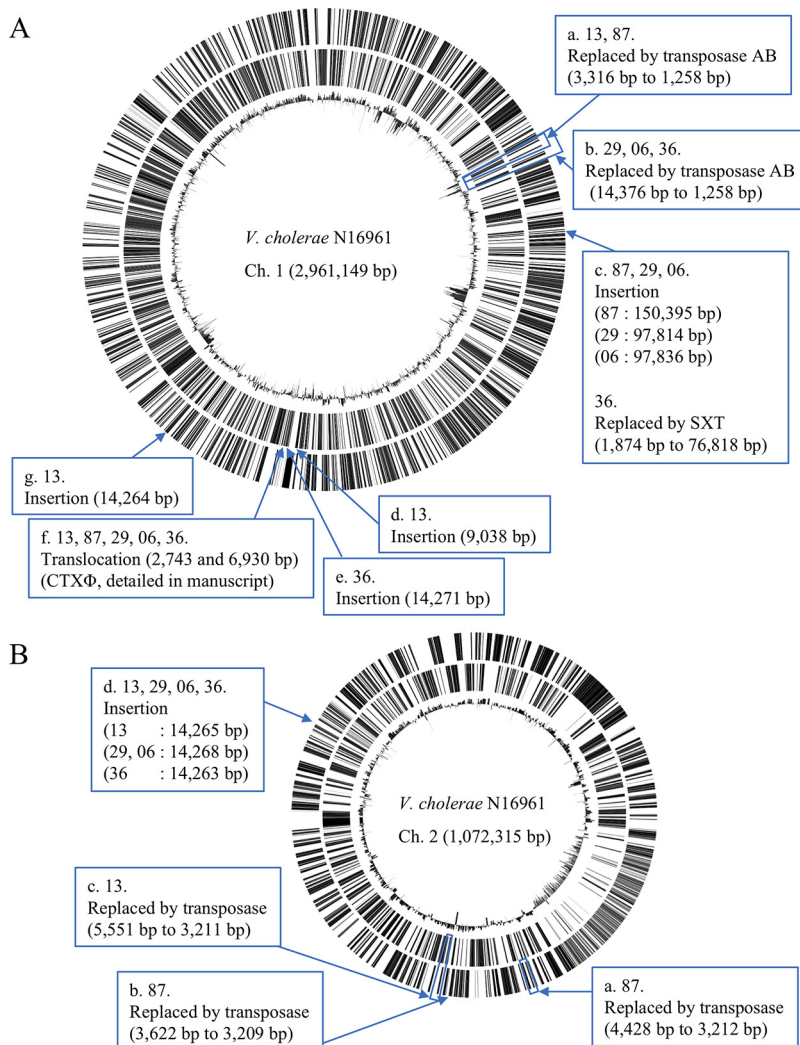


FIG 2 Structural variations in the chromosomes of *V. cholerae*. Replacements, insertions, and translocations of >2,000 bp compared with the N16961 genomic sequences, suggested on the basis of complete genomic sequences obtained in this study and confirmed by PCR, are illustrated. Circular chromosomal maps having genes on the plus strand, those with genes on the minus strand, and GC percent (from outside to inside) were generated using Civi (Circular Visualization for Microbial Genomes [60]). A, larger chromosome; B, smaller chromosome.

(referred to here as strain 87), isolated in 2007 and 2009, respectively, represented lineage 1 and were predominant until 2009 (15). IDH-03329 (referred to here as strain 29), isolated in 2010, and IDH-03506 (referred to here as strain 06) and BCH-01536 (referred to here as strain 36), isolated in 2011, belong to sublineages III and IV, respectively, of lineage 2. Lineage 2 sublineage III strains were transient in Kolkata and observed only in 2010. Thereafter, sublineage IV strains of lineage 2 became predominant.

Long-read genomic sequences of these strains were obtained using Oxford Nanopore MinION, and the nucleotide sequences were polished by short reads obtained by Illumina sequencing (15). Then, the complete genomic sequences were assembled and their chromosomal structures were compared with that of *V. cholerae* N16961, a prototype El Tor strain. The detected structural variations were verified through PCR amplification (data not shown). The confirmed differences of >2,000 bp are summarized in Fig. 2 and Table 1. The previously identified variations in the VSP-II genetic island, in which 3,343-bp and 14,376-bp regions were replaced by transposase genes in lineages 1 and 2, respectively, were confirmed in this study (15) (Fig. 2A, boxes a and b). Various integral and conjugative elements

TABLE 1 Genomic variations in recent *V. cholerae* isolates over 2,000 bp in size

| Position in Fig. 2 | Position in N16961 genome | | ORFs at position | Altered type | Altered strains | Size | | Description of acquired sequence |
|---------------------------|---------------------------|-----------|--------------------|---------------|--------------------|--------|----------|--|
| | Start | End | | | | Lost | Acquired | |
| Chr. 1^a | | | | | | | | |
| a | 529,128 | 532,472 | VC0495 to VC0500 | Replacement | 13, 87 | 3,343 | 1,258 | VSP-II, transposase |
| b | 529,128 | 543,505 | VC0495 to VC0512 | Replacement | 29, 06, 36 | 14,376 | 1,257 | VSP-II, transposase |
| c | 703,929 | 703,944 | VC0659 | Insertion | 87 | | 150,395 | SXT element |
| c | 703,923 | 703,944 | VC0659 | Insertion | 29 | | 97,814 | SXT element |
| c | 703,929 | 703,944 | VC0659 | Insertion | 06 | | 97,836 | SXT element |
| c | 702,055 | 703,930 | VC0658 to VC0659 | Replacement | 36 | 1,874 | 76,818 | SXT element |
| d | 1,545,050 | 1,545,057 | VC1446 | Insertion | 13 | | 9,038 | Transposase |
| e | 1,568,642 | 1,568,643 | VC1548 (zot) | Insertion | 36 | | 14,271 | Includes genes for transposase and phage integrase |
| f | | | | Translocation | 13, 87, 29, 06, 36 | | | CTXΦ and RS1, detailed here |
| g | 1,817,850 | 1,817,852 | VC1683 | Insertion | 13 | | 14,264 | Includes genes for transposase and phage integrase |
| Chr. 2 | | | | | | | | |
| a | 479,414 | 483,843 | VCA0543 to VCA0545 | Replacement | 87 | 4,428 | 3,212 | Transposase |
| b | 556,942 | 560,565 | VCA0623 to VCA0625 | Replacement | 87 | 3,622 | 3,209 | Transposase |
| c | 567,157 | 572,709 | VCA0629 to VCA0638 | Replacement | 13 | 5,551 | 3,211 | Transposase |
| d | 634,743 | 634,744 | VCA0695 | Insertion | 13 | | 14,265 | Includes genes for transposase and phage integrase |
| d | 634,222 | 634,223 | VCA0695 | Insertion | 29 | | 14,268 | Includes genes for transposase and phage integrase |
| d | 634,743 | 634,744 | VCA0695 | Insertion | 06 | | 14,268 | Includes genes for transposase and phage integrase |
| d | 634,743 | 634,744 | VCA0695 | Insertion | 36 | | 14,263 | Includes genes for transposase and phage integrase |

^aChr., chromosome.

of approximately 150, 98, and 77 kbp were found in isolates 87, 29/06, and 36, respectively; these findings were consistent with those published in a recent report (22) (Fig. 2A, box c). Insertions of 9,038 bp, 14,271 bp, and 14,264 bp fragments including a gene encoding transposase in strains 13, 36, and 13, respectively, were identified (Fig. 2A, boxes d, e, and g). The DNA fragment was inserted in strain 36 into *zot*, a gene in the CTX Φ prophage genome, and consequently, the gene was divided (Fig. 2A, box e). The 14-kbp (approximately) sequences inserted in strains 13 and 36 were nearly identical to the origin-proximal regions, including VC0175 to VC0185, suggesting duplication and insertion of the fragment into the distal region (Fig. 2A, boxes e and g).

In addition to these insertions and replacements, translocation within the CTX Φ region in all recent isolates compared with the N16961 strain was detected (Fig. 2A, box f). The analysis of this structural difference is described in detail below. In the smaller chromosome, three replacements by a transposase-encoding gene (Fig. 2B, boxes a, b and c) and an insertion of approximately 14-Kbp fragment in strains 13, 29, 06, and 36 were detected (Fig. 2B, box d). This 14-kbp fragment was also almost identical to the region VC0175 to VC0185 in the chromosome 1 (Fig. 2A, boxes e and g), indicating duplication and insertion from larger to smaller chromosomes. In summary, the results indicated that the chromosomes of pathogenic *V. cholerae* strains were frequently replaced with mobile genetic elements and were highly diverse even in spatio-temporally close clinical isolates.

Alteration of CTX Φ prophage arrays. We next focused on the alteration of the CTX Φ prophage array among the identified structural differences (Fig. 2; Table 1). The CTX Φ prophage genome in the El Tor biotype strains is usually found in tandem and/or followed by the related genetic element known as RS1, and this tandem array is essential for the replication and induction of CTX Φ (17) (Fig. 1A to D). In brief, the CTX Φ prophage genome was replicated by nicking two Ig-1 sites of CTX Φ and the following element by either tandem CTX Φ or RS1, i.e., Ig-1 upstream and downstream of the CTX Φ genome (Fig. 1A). The complete genomic sequences obtained in this study and after PCR confirmation indicated that all recent isolates possessed intact gene sets of CTX Φ prophage and RS1. However, RS1 was located at the upstream end of the CTX Φ genome, in contrast to the prototype El Tor strains (Fig. 1A and E). These arrays of the CTX Φ region possessed Ig-1, a nicking site for rolling-circle replication, only at the upstream end of the prophage genome. This observation suggests that the recent *V. cholerae* epidemic strains have lost the ability to replicate the CTX Φ genome and have led to the subsequent production of infectious phage particles. To confirm this possibility, a circular replication product of CTX Φ phage was specifically detected using PCR (Fig. 3A). The prototype El Tor type strain N16961 produced the replication product with and without mitomycin C induction (Fig. 3B). However, no such replication was detected in all recent isolates, even in the mitomycin C-induced condition (Fig. 3B). These results confirmed that recent *V. cholerae* strains are incapable of replicating the CTX Φ prophage genome.

Factors required for replication. It was reported that *rstA* is the only CTX Φ gene required for its replication in *V. cholerae* (19). We next investigated whether *rstA* is sufficient for the replication in the absence of CTX Φ and specific elements of *V. cholerae*. *rstA* was cloned into the plasmid pET-21a, and Ig-1 sequences were inserted upstream and downstream of the gene (Fig. 4A). *rstA* expression was induced in *E. coli* BL21 using IPTG (isopropyl- β -D-thiogalactopyranoside), and circular rolling-circle replication products were detected using PCR with the primers in the inverse direction (Fig. 4A and B). The *V. cholerae* genomic sequence was inserted instead of Ig-1 as a negative control. The replication was detected in *Escherichia coli* only in the presence of both *rstA* expression and Ig-1 (Fig. 4C). These results indicated that the two Ig-1 nicking sites as well as *rstA* expression were necessary and sufficient in *V. cholerae* and CTX Φ -specific elements for replication. Because all strains used in this study possessed Ig-1, *rstA*, and its upstream sequence identical to those of *V. cholerae* N16961, *rstA* expression levels in these strains were compared. *rstA* was mainly expressed in the exponential growth phase, and the expression decreased in the stationary phase in all tested *V. cholerae*

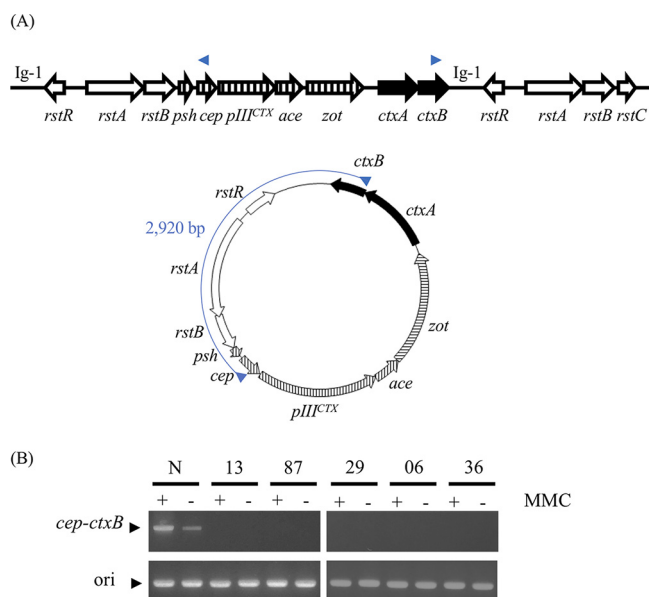


FIG 3 Detection of rolling-circle replication products of the CTXΦ prophage genome. Primers were designed in *cep* (P17) and *ctxB* (P16) in the CTXΦ prophage genome in inverse directions (A, top). DNA fragments of 2,920 bp were amplified only from circular rolling-circle replication products (A, bottom). (B) Amplified fragments from CTXΦ replication products and origin proximal genomic region as a control. MMC, mitomycin C induction; N, strain N16961.

strains (data not shown). Although the relative expression levels of recent isolates in the growth phase compared with N16961 showed some variation (0.5- to 1.3-fold), comparable *rstA* expression levels in all strains were confirmed (Fig. 5). These results indicated that all strains used in the present study possessed the necessary genetic elements

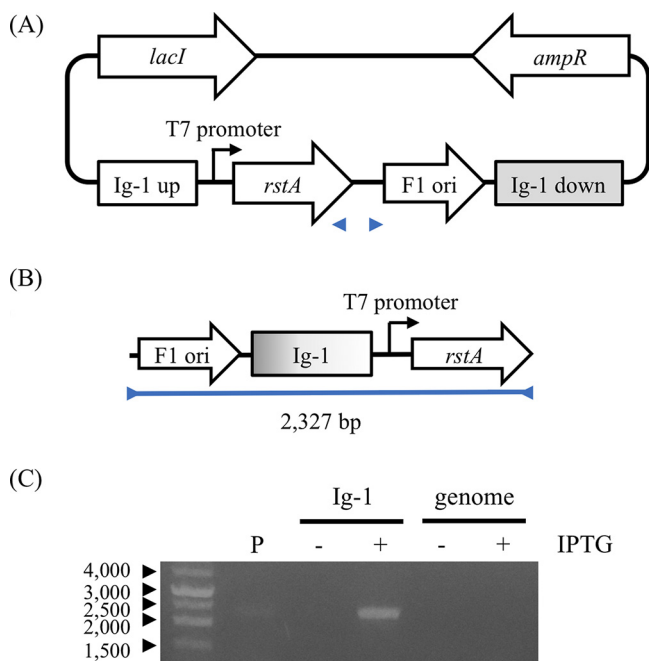


FIG 4 Reconstitution of rolling-circle replication by RstA in *E. coli*. *rstA* was cloned into pET-21a under the control of the T7 promoter. The *Ig-1* regions of CTXΦ and RS1 were inserted upstream and downstream of *rstA*, respectively (A). The circular rolling-circle replication product was detected using primers in inverse directions (B and C). P, empty plasmid; genome, genomic sequences of *V. cholerae* instead of *Ig-1* were cloned into the plasmid; IPTG, isopropyl-β-D-thiogalactopyranoside induction of *rstA* expression.

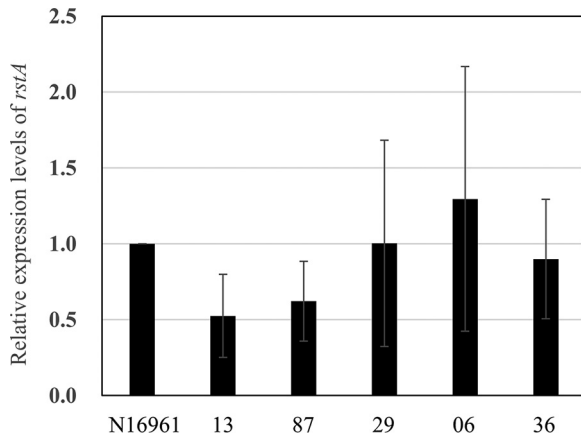


FIG 5 Expression levels of *rstA*. mRNA of *rstA* was quantified by reverse transcription and qPCR. Expression levels relative to that of N16961 are shown. Data points are averages from three independent experiments. Error bars represent standard errors.

for CTX Φ replication, and thus, the altered prophage array structure was supposedly responsible for the inability to replicate.

Impact of CTX Φ replication. We estimated the number of CTX Φ phage produced from a single *V. cholerae* bacterium. Because CTX Φ is not a plaque-forming phage and phage particles are not detected as PFU, its genomic DNA was quantified instead of phage particles. All strains used in this study possessed a single copy of *ctxA* in the genome (Fig. 1A and E). Therefore, the DNA fragment of *ctxA* from an equal amount of extracted DNA was compared using quantitative PCR (qPCR) for the CTX Φ replication of positive and negative strains (Fig. 6). In the CTX Φ replication-positive N16961 strain, the amount of *ctxA* fragment increased slightly during stationary phase compared to that in the exponential growth phase. All the negative isolates from CTX Φ replication exhibited approximately half of the amount of the *ctxA* fragment in N16961 (Fig. 6). It is not clear whether a small cell population replicated the CTX Φ prophage genome many times or most cells replicated it only a few times. Nonetheless, these results indicated that prototype

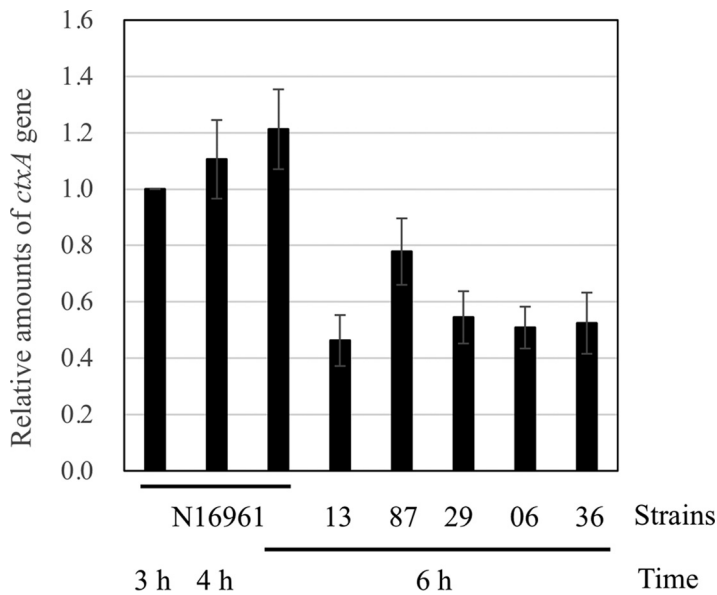


FIG 6 Quantification of *ctxA*. DNA fragment of *ctxA* was quantified, and the relative amounts are shown. “Time” indicates the number of hours of incubation. Data points are averages from five independent experiments. Error bars represent standard errors.

TABLE 2 *V. cholerae* strains and CTXΦ sequences from the literature cited in the study

| Strain | Yr | Location | CTXΦ structure | Biotype | Genome accession no. | Reference |
|-------------|------|-----------------------------------|----------------|----------------|---------------------------------|-----------|
| A1M | 1956 | Bangkok, Thailand | B1 | El Tor, wave 1 | | 23 |
| C5 | 1957 | Makassar, Indonesia | B2 | El Tor, wave 1 | GCA_001887395.1 | 38 |
| C7 | 1961 | Sulawesi, Indonesia | A10 | El Tor, wave 1 | | 23 |
| C1 | 1961 | Sulawesi, Indonesia | A11 | El Tor, wave 1 | | 23 |
| J6 | 1961 | Sarawak, Malaysia | A7 | El Tor, wave 1 | | 23 |
| J9 | 1961 | Sarawak, Malaysia | A7 | El Tor, wave 1 | | 23 |
| C2 | 1961 | Sulawesi, Indonesia | A7 | El Tor, wave 1 | | 23 |
| P2 | 1961 | Philippines | A9 | El Tor, wave 1 | | 23 |
| P3 | 1961 | Philippines | A9 | El Tor, wave 1 | | 23 |
| P4 | 1961 | Philippines | A9 | El Tor, wave 1 | | 23 |
| P16 | 1961 | Philippines | A9 | El Tor, wave 1 | | 23 |
| P18 | 1961 | Philippines | A9 | El Tor, wave 1 | | 23 |
| P31 | 1961 | Philippines | A9 | El Tor, wave 1 | | 23 |
| P7 | 1961 | Philippines | B1 | El Tor, wave 1 | | 23 |
| E9120 | 1961 | Indonesia | B2 | El Tor, wave 1 | GCA_001887655.1 | 39 |
| M25 | 1962 | Moji, Japan | A4 | El Tor, wave 1 | | 23 |
| CRC711 | 1962 | Kolkata, India | B1 | El Tor, wave 1 | GCA_001887435.1 | 40 |
| 193 | 1962 | Taiwan | B1 | El Tor, wave 1 | | 23 |
| 341 | 1962 | Taiwan | B1 | El Tor, wave 1 | | 23 |
| T10 | 1962 | Taiwan | B1 | El Tor, wave 1 | | 23 |
| T100 | 1962 | Taiwan | B1 | El Tor, wave 1 | | 23 |
| CRC1106 | 1964 | Kolkata, India | B2 | El Tor, wave 1 | GCA_001887455.1 | 40 |
| O395 | 1965 | India | B3 | Classical | | 17 |
| A19 | 1971 | Bangladesh | A1 | El Tor, wave 1 | GCA_001250235.2 | 14 |
| E506 | 1973 | Texas, USA | A8 | Classical | GCA_001887475.1 | 41 |
| N16961 | 1975 | Bangladesh | A1 | El Tor, wave 1 | GCA_003063785.1 | 42 |
| P27459 | 1976 | Bangladesh | A4 | El Tor, wave 1 | GCA_013085125.1 | 42 |
| M2140 | 1977 | Australia | A9 | Classical | GCA_001887635.1 | 43 |
| E7946 | 1978 | Bahrain | A3 | El Tor, wave 1 | GCA_013085165.1 | 42 |
| C6706 | 1991 | Peru | A1 | El Tor, wave 1 | GCA_009763945.1 | 44 |
| C6709 | 1991 | Peru | A1 | El Tor, wave 1 | GCA_013085105.1 | 45 |
| A1552 | 1992 | Traveler from Peru to California | A1 | El Tor, wave 1 | GCA_003097695.1 | 46 |
| IEC224 | 1994 | Belém, Brazil | A1 | El Tor, wave 1 | GCA_000250855.1 | 47 |
| V060002 | 1997 | Patient who traveled to Indonesia | A9 | El Tor, wave 2 | GCA_003574155.1 | 48 |
| FJ147 | 2005 | China, Fujian | A1 | El Tor, wave 3 | GCA_000963555.1 | 49 |
| 3528-08 | 2008 | Texas, USA | A2 | El Tor, wave 2 | GCA_009762895.1 | 50 |
| 3566-08 | 2008 | New Jersey, USA | A5 | El Tor, wave 2 | GCA_009763105.1 | 51 |
| MS6 | 2008 | Thailand-Myanmar | A6 | El Tor, wave 1 | GCA_000829215.1 | 52 |
| 3569-08 | 2008 | Louisiana, USA | A8 | El Tor, wave 2 | GCA_009762985.1 | 53 |
| 2010EL-1786 | 2010 | Artibonite, Haiti | B1 | El Tor, wave 3 | GCA_009665515.1 | 53 |
| H1 | 2010 | Haiti | B1 | El Tor, wave 3 | GCA_000275645.1 | 53 |
| KW3 | 2010 | Haiti | B1 | El Tor, wave 3 | GCA_001318185.1 | 54 |
| TSY216 | 2010 | Tak, Thailand | B1 | El Tor, wave 3 | GCA_001045415.1 | 55 |
| DRC-193A | 2011 | Congo | B1 | El Tor, wave 3 | GCA_013085145.1 | 56 |
| 2012EL-2176 | 2012 | Haiti | B1 | El Tor, wave 3 | GCA_000765415.1 | 57 |
| HC1037 | 2014 | Jacmel, Haiti | B1 | El Tor, wave 3 | GCA_002946655.1 | 58 |
| CTMA_1441 | 2015 | Mutwanga, Congo | B1 | El Tor, wave 3 | GCA_009799825.1 | 59 |

El Tor strain produces CTXΦ phage at number comparable to that of the cell population and that its impact on the dissemination of cholera cannot be ignored.

Variation in CTXΦ arrays of known *V. cholerae* strains. The CTXΦ array patterns detected in 52 *V. cholerae* strains are depicted in Table 2 and Fig. 7. Data regarding the year of isolation and the complete genomic sequence or CTXΦ structures are available in the literature (23). Fourteen CTXΦ array patterns were identified from strains isolated between 1956 and 2015 from Asia, Africa, Latin America, and North America (Fig. 7; Table 2). Among the 14 CTXΦ array variations, 11 possessed Ig-1 at both the upstream and downstream ends of CTXΦ prophage genome (indicated with an “A” in Fig. 7), suggesting that these strains can produce infectious virions, whereas 3 CTXΦ arrays demonstrated defective replication when the structure was observed (indicated with a “B” in Fig. 7). Of note, non-CTXΦ-producing strains were isolated in 1965 and earlier, but, later

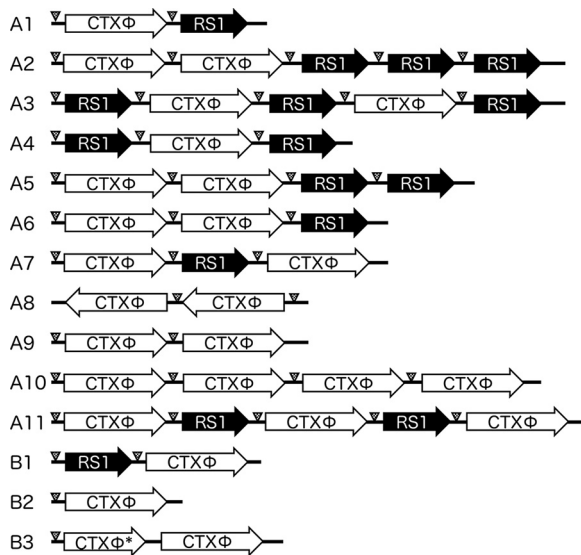


FIG 7 Variations in CTXΦ arrays in pathogenic *V. cholerae* isolates. The CTXΦ arrays of pathogenic *V. cholerae* strains listed in Table 2 are shown. Arrows labeled “CTXΦ” and “RS1” indicate the CTXΦ genome in the *rstR*-to-*ctxB* direction and the RS1 element in the *rstR*-to-*rstC* direction, respectively (Fig. 1A). The right side of the displayed array is followed by the *rtxA* gene. *, truncated CTXΦ genome lacking sequence downstream from the internal region of *cep*, as shown in Fig. 1 (classical). Triangles, Ig-1 region (167 bp), which is required for rolling-circle replication (20). A and B indicate the CTXΦ arrays, which are expected to be capable and incapable of replication, respectively.

on, CTXΦ-producing strains were reported to be more dominant worldwide for over 3 decades (Fig. 8; Table 2). The strain used in this study, i.e., those with the non-CTXΦ-producing CTXΦ structure type B1, appeared in 2007 in India, and this type of strain became predominant after 2009 in Asia, Africa, and Latin America (Fig. 8; Table 2). In summary, these data suggest that *V. cholerae* epidemic strains did not produce CTXΦ phage during the sixth and early seventh pandemics, but the pattern shifted to the CTXΦ-producing strains in the 1970s. This probably generated new pathogenic *V. cholerae* strains in the environment through CTXΦ phage infection during these periods, which lasted for over 3 decades. However, the pandemic strains were again found to have lost the ability to produce CTXΦ phage particles around 2010, indicating that the observed dissemination patterns are at a critical stage during the ongoing cholera pandemic.

DISCUSSION

V. cholerae is generally found in an aquatic environment, where it acquires unique characteristic features that makes it better adapted to a particular environment through the uptake of genetic molecules from natural resources, either through transformation or via interaction with other inhabitants (4). In this manner, the bacteria communicate with

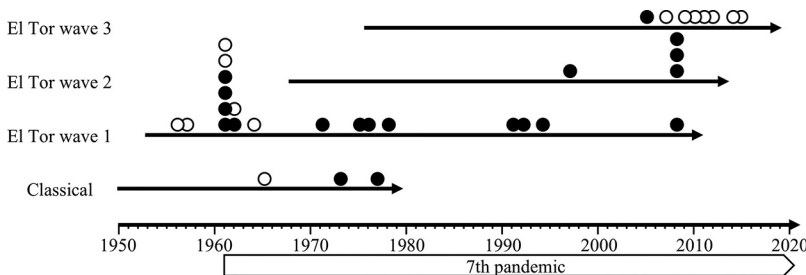


FIG 8 Schematic representation of CTXΦ productivity and years of isolation of *V. cholerae*. Years in which *V. cholerae* strains with replicative (black circle) and nonreplicative (white circle) CTXΦ arrays were isolated are indicated (Table 2). The biotypes and waves of each strain were determined on the basis of *ctxB*, *rstR*, and *rstA* genotypes (14).

the toxigenic CTX Φ phage and integrate the genomic constituents of the phage irreversibly into their genomes so as to gain the toxic components of the phage genome, mainly *ctxA* and *ctxB*; therefore, the risk of this disease progression in humans has invariably increased (2).

The two naturally occurring *V. cholerae* biotypes possess CTX Φ phage-integrated genomes but with different arrangements and cellular functions (17). In recent years, novel variants of *V. cholerae* O1 have been found to emerge with altered *ctxB* genotypes and with higher pathogenic potency (5, 24). Past reports suggested that the classical *V. cholerae* strains could not produce virions, as they would not yield extrachromosomal CTX Φ DNA (17). Comparative genomics revealed that, despite having functional genes for the replication and production of phage particles, classical strains were unable to replicate the CTX Φ phage genome only because of the structural deficiencies in the CTX Φ prophage array (17). However, on the emergence of the seventh pandemic, the El Tor strains were found to possess functional CTX Φ phage genomes that could produce transducible virions (25). With time, different El Tor strains (atypical El Tor) were found to emerge from different places worldwide with modified genetic makeup of the CTX Φ prophage (5). These atypical El Tor strains were found to arise on the prototype El Tor genomic background only by replacing CTX Φ phages of different types (21). Thus, the wave 2 El Tor strains possessed tandem repeats of classical-CTX Φ -like prophages on their second chromosome (14). Other CTX Φ prophage-containing pathogenic variants of *V. cholerae* included *V. cholerae* O139, which harbored an extra copy of a different CTX Φ prophage located at the downstream end of the preexisting El Tor type CTX Φ prophage on the first chromosome (26). Faruque et al. demonstrated the presence of a different type of CTX Φ prophage array in the isolates of the Mozambique variant El Tor strains (27). These strains contained 2 copies of the classical CTX Φ prophages in the second chromosome, but they were unable to produce virions.

In this study, we demonstrated that recent *V. cholerae* clinical strains isolated in Kolkata were incapable of replicating the CTX Φ prophage genome and hence were not responsible for the production of infectious virions. Because CTX Φ is not a plaque-forming phage, genetic engineering of pathogenic *V. cholerae* to introduce an antibiotic-resistant gene into the CTX Φ genome is required to assay phage particle productivity (6). These analyses are expected to further confirm the conclusions of the present study. Nevertheless, the data in the present study strongly suggest that the recent *V. cholerae* epidemic strains do not produce infectious virions. In strain 36, a gene in the CTX Φ genome, *zot*, was disrupted by the insertion of a 14,271-bp fragment that included a transposase-encoding gene (Fig. 2A, box e). *Zot* is required for packaging and secretion of the phage as well as possessing enterotoxin activity (21). It may be suggested that the disruption of *zot* was allowed because phage secretion was no longer required in the strain incapable of replicating the CTX Φ genome.

The infection of *V. cholerae* O1 cells by CTX Φ requires toxin-coregulated pilus (TCP) as the receptor (6). Biogenesis of TCP is dependent on the *tcp* operon in *Vibrio* pathogenicity island 1 (VPI-1) on larger chromosomes. The first gene of the operon, *tcpA* encodes the major pilin subunit (28). Thus, the *tcp*-positive *V. cholerae* O1 strains are potential hosts for the CTX Φ infection to generate epidemic strains. We attempted to isolate *V. cholerae* O1 strains from lakes, ponds, and rivers in Kolkata, India, between 2014 and 2016 several times and characterized the strains. During this analysis, only one *ctxA*-positive strain was isolated, whereas 181 *tcpA*-positive strains were identified (data not shown). These observations suggest that many more potential host cells for the CTX Φ infection exist than the pathogenic *V. cholerae* O1 strains in environmental water. Therefore, the cholera pandemic caused by the CTX Φ -producing strains disseminated CTX Φ phage particles into the environment and possibly generated new pathogenic *V. cholerae* O1 strains. Thus, the results of the present study suggest that, during the seventh pandemic, the spread of cholera acquired a secondary disseminating route in which the secreted CTX Φ phage particles generated new pathogenic *V. cholerae* O1 strains in the environment (Fig. 8). It was reported that the El Tor type strains were less

virulent than the classical type strains, but the recent variant exhibited increased production of toxins (29). It can be concluded that non-CTX Φ -producing strains with higher virulence were disseminated by the fecal-oral route by causing severe diarrhea and that CTX Φ -producing strains with lower virulence were spread both by the fecal-oral route and by the generation of new pathogenic strains in the environment because of CTX Φ infection. Thus, the prototype El Tor strains required the spread of CTX Φ productivity, while the classical type and the recent variant did not. On the other hand, CTX Φ productivity may be one of the reasons why the seventh pandemic continued for a longer period, i.e., for over half a century, than other pandemics. If this is the case, the appearance of the non-CTX Φ -producing El Tor strain brought a significant change that can be of great help to restrict the dissemination of *V. cholerae* and cholera worldwide. Epidemiological studies shall further confirm and reveal the effects of the change in CTX Φ productivity of *V. cholerae* found in the present study.

In addition, *V. cholerae* El Tor strains, which were more stable in the environment but less pathogenic than classical strains, acquired virulence properties of the hypervirulent classical strains in recent years. The first report of *V. cholerae* El Tor strains mentioned the acquisition of classical *ctxB* in the El Tor genomic background in the strains of Kolkata during the 1990s (10). Thereafter, the appearance of a new variant hyperpathogenic *ctxB* genotype (*ctxB7*) was first observed in the isolates of Kolkata during 2006, which attracted the attention of scientists after the Haitian cholera outbreak of 2010 (13). It was recently discovered that one of the major phenotypic characteristics of the classical biotype strain, i.e., polymyxin B sensitivity, was also transmitted to the El Tor biotype strains circulating in Kolkata (30, 31). A similar finding was made in this study with regard to the characteristic of the classical biotype strain, i.e., the inability to produce CTX Φ virions like the classical strains, although it involved a different mechanism. Thus, the recent trend of gaining classical biotype traits by El Tor biotype strains indicates that the new variant *V. cholerae* El Tor strains with hyperpathogenic characteristics adapt slowly to the environment and also evolve slowly; such strains can prove fatal to human beings and may lead to a more severe cholera outbreak situation in the near future worldwide.

MATERIALS AND METHODS

Strains used in the study. The strains were isolated from patients with cholera in Kolkata, India, between 2007 and 2011 and were phylogenetically analyzed as described previously (15). Strains IDH-00113 (referred to here as strain 13) and IDH-02387 (strain 87) isolated in 2007 and 2009, respectively, belong to lineage 1, which was predominant in Kolkata until 2009. Strain IDH-03329 (strain 29), isolated in 2010, as well as IDH-03506 (strain 06) and BCH-01536 (strain 36), isolated in 2011, were classified into lineage 2, sublineages III and IV, respectively. It was revealed that lineages 1 and 2 were concurrently prevalent between 2007 and 2009, while lineage 2-III appeared in 2010, followed by the predominance of lineage 2-IV in 2011 and later (15).

Plasmid construction. The oligonucleotide primers used in the study are listed in Table 3. To construct the *rstA* expression plasmid with Ig-1 or control genomic sequence, the primer pairs P1/P2, P3/P4, P5/P6, and P7/P8 were used to amplify the Ig-1 of CTX Φ (Ig-1 up), Ig-1 of RS1 (Ig-1 down), an N16961 genomic region of approximately 1.5 Mbp (1.5 genome), and a 1.1-Mbp (1.1 genome) region of the larger chromosome, respectively. Inverse PCR was performed using the primer pair P9/P10 and pET-21a as a template, followed by ligation using a seamless ligation-independent cell lysate (32) with the Ig-1 up or 1.5 genome fragment. Inverse PCR was performed again using the resulting plasmids as a template, with the primer pair P11/P12 ligated with the Ig-1 down or 1.1 genomic fragment. The resulting plasmids were digested using NdeI/XhoI and ligated with an NdeI/XhoI-digested *rstA* fragment, which was amplified with primer pair P13/P14. Constructed plasmids were verified via sequencing. The plasmids were propagated in *Escherichia coli* DH5 α , and *rstA* expression was induced in *E. coli* BL21.

Genome sequencing. The genomic DNA of *V. cholerae* strains was extracted using the DNeasy blood and tissue kit (Qiagen) as per the manufacturer's instructions. Nanopore-based DNA sequencing was performed using the Native Barcoding Expansion 1-12 (EXP-NBD104; Oxford Nanopore Technologies [ONT, Oxford, UK]) and a ligation sequencing kit (SQK-LSK109; ONT), and DNA was loaded onto the MinION sequencing apparatus flow cell (R9.4.1; FLO-MIN106D; ONT) as per the manufacturer's instructions. The raw reads were base called (i.e., electronic signals were converted to the corresponding base sequence of the DNA strand) using Albacore software (ONT). The DNA sequence reads obtained were separated on the basis of the barcode sequence of each strain, and the adapters were trimmed off by using the Porechop software (33). Circular chromosomal sequences were assembled from the obtained reads with at least 30-fold coverage of the *V. cholerae* genome using flye (34) or unicycler (35), and the sequences were then polished by short reads (15) using Pilon software (36).

TABLE 3 Primers used in this study

| Name | Sequence (5'→3') |
|------|-------------------------------------|
| P1 | TGCGTCCGGCGTAGACTAAACCTAGAGACAAAATG |
| P2 | TCGAGATCTCGATCCAGCATCTAAATCATGGTGC |
| P3 | ACTTTTCGGGGAAATCAAACATGTATTACTGCAAG |
| P4 | AGGGGTTCCGCGCACAGCATCTAAATCATGGTGC |
| P5 | TGCGTCCGGCGTAGATCTTGAATTGAATTATCCG |
| P6 | TCGAGATCTCGATCCTCTAAGTCCAACCTCCTCGC |
| P7 | ACTTTTCGGGGAAATAATGGACGTATTCTGTCACC |
| P8 | AGGGGTTCCGCGCACGACGTCAGGTCAGGTTGATC |
| P9 | GGATCGAGATCTCGATCCCG |
| P10 | TCTACGCCGGACGCATCGTG |
| P11 | ATTTCCCGAAAAGTGCCAC |
| P12 | GTGCGCGAACCCTATTTG |
| P13 | GGAATCCATATGAAAAGCAGATTTTCAC |
| P15 | CCGCTCGAGATCACCCATAATTCATCAATTAAC |
| P16 | TGAAAGGATGAAGGATACCC |
| P17 | ACCGTATCTTTACTGGTGCC |
| P18 | CTCCAAGCGTTCATCATG |
| P19 | GCGCATAAGTCCGATTTGTC |
| P20 | GGTACTGAAGGGTCTGGATG |
| P21 | CGATGCTTTACAGTAACCTGC |
| P22 | CAGATTCTAGACCTCCTGATG |
| P23 | TACACCTAGACTTTGGGTTT |

Detection of structural variation in genomes. The obtained genomic sequences were compared with those of *V. cholerae* N16961 by 500 kbp each using Easyfig software (<https://mjsull.github.io/Easyfig/>). The structural variants were further compared with the help of the dot plot using BLAST. These variants were verified using PCR by amplifying the upstream and downstream ends of the altered region (data not shown).

Rolling-circle replication. *V. cholerae* strains were incubated in alkaline peptone water at 37°C. To this, 20 ng/ml of mitomycin C was added to induce CTX Φ prophage (37) at an optical density at 600 nm (OD₆₀₀) of 0.2. After 7 h of initiation of incubation, total DNA was extracted using the phenol-chloroform method. The total DNA was adjusted to 100 ng/ μ l and used as a template for PCR with the primer pair P16/P17.

Relative expression levels of *rstA*. Total RNA was extracted using the Quick-RNA MiniPrep Plus kit (Zymo Research) as per the manufacturer's instructions. Sixteen nanograms of extracted RNA was subjected to reverse transcription with random primers using iScript reverse transcription supermix for performing reverse transcription-quantitative real-time PCR (RT-qPCR) analysis (Bio-Rad). cDNA for *rstA* and the gene VC0015 (encoding gyrase) were quantified by qPCR (PowerTrack SYBR green master mix; Thermo Fisher) with the primer pairs P18/P19 and P20/P21, respectively. VC0015 was used to normalize the expression level of *rstA*.

Quantification of *ctxA* DNA. The *V. cholerae* strains were incubated in alkaline peptone water at 37°C for the indicated time periods from 3 to 6 h. DNA was extracted and adjusted to 0.6 ng/ μ l and then subjected to qPCR with the primer pair P22/P23. The relative quantity of *ctxA* DNA with respect to the N16961 strain at 3 h was determined.

Data availability. Nucleotide sequence data for larger and smaller chromosomes of strains IDH-00113, IDH-02387, IDH-03329, IDH-03506, and BCH-01536 generated in this study are available in the DDBJ database under accession numbers [AP024549/AP024550](https://doi.org/10.1128/10.1128/MMBR.62.4.1301-1314.1998), [AP024551/AP024552](https://doi.org/10.1128/10.1128/MMBR.62.4.1301-1314.1998), [AP024553/AP024554](https://doi.org/10.1128/10.1128/MMBR.62.4.1301-1314.1998), [AP024555/AP024556](https://doi.org/10.1128/10.1128/MMBR.62.4.1301-1314.1998), and [AP024547/AP024548](https://doi.org/10.1128/10.1128/MMBR.62.4.1301-1314.1998), respectively.

ACKNOWLEDGMENTS

This work was supported by JSPS KAKENHI grant 18K07126 to D.I. and AMED under grant 20wm0225012s0101 to D.I.

REFERENCES

- Colwell RR. 1996. Global climate and infectious disease: the cholera paradigm. *Science* 274:2025–2031. <https://doi.org/10.1126/science.274.5295.2025>.
- Faruque SM, Albert MJ, Mekalanos JJ. 1998. Epidemiology, genetics, and ecology of toxigenic *Vibrio cholerae*. *Microbiol Mol Biol Rev* 62:1301–1314. <https://doi.org/10.1128/MMBR.62.4.1301-1314.1998>.
- Blake PA, Allegra DT, Snyder JD, Barrett TJ, McFarland L, Caraway CT, Feeley JC, Craig JP, Lee JV, Puhr ND, Feldman RA. 1980. Cholera—a possible endemic focus in the United States. *N Engl J Med* 302:305–309. <https://doi.org/10.1056/NEJM198002073020601>.
- Kaper JB, Morris JG, Jr, Levine MM. 1995. Cholera. *Clin Microbiol Rev* 8:48–86. <https://doi.org/10.1128/CMR.8.1.48>.
- Safa A, Nair GB, Kong RY. 2010. Evolution of new variants of *Vibrio cholerae* O1. *Trends Microbiol* 18:46–54. <https://doi.org/10.1016/j.tim.2009.10.003>.
- Waldor MK, Mekalanos JJ. 1996. Lysogenic conversion by a filamentous phage encoding cholera toxin. *Science* 272:1910–1914. <https://doi.org/10.1126/science.272.5270.1910>.
- Alam M, Islam MT, Rashed SM, Johura FT, Bhuiyan NA, Delgado G, Morales R, Mendez JL, Navarro A, Watanabe H, Hasan NA, Colwell RR, Cravioto A. 2012.

- Vibrio cholerae* classical biotype strains reveal distinct signatures in Mexico. *J Clin Microbiol* 50:2212–2216. <https://doi.org/10.1128/JCM.00189-12>.
8. Ceccarelli D, Spagnoletti M, Bacciu D, Cappuccinelli P, Colombo MM. 2011. New *V. cholerae* atypical El Tor variant emerged during the 2006 epidemic outbreak in Angola. *BMC Microbiol* 11:130. <https://doi.org/10.1186/1471-2180-11-130>.
 9. Nair GB, Faruque SM, Bhuiyan NA, Kamruzzaman M, Siddique AK, Sack D. 2002. New variants of *Vibrio cholerae* O1 biotype El Tor with attributes of the classical biotype from hospitalized patients with acute diarrhea in Bangladesh. *J Clin Microbiol* 40:3296–3299. <https://doi.org/10.1128/jcm.40.9.3296-3299.2002>.
 10. Raychoudhuri A, Patra T, Ghosh K, Ramamurthy T, Nandy RK, Takeda Y, Nair GB, Mukhopadhyay AK. 2009. Classical *ctxB* in *Vibrio cholerae* O1, Kolkata, India. *Emerg Infect Dis* 15:131–132. <https://doi.org/10.3201/eid1501.080543>.
 11. Son MS, Megli CJ, Kovacicova G, Qadri F, Taylor RK. 2011. Characterization of *Vibrio cholerae* O1 El Tor bio-type variant clinical isolates from Bangladesh and Haiti, including a molecular genetic analysis of virulence genes. *J Clin Microbiol* 49:3739–3749. <https://doi.org/10.1128/JCM.01286-11>.
 12. Weill FX, Domman D, Njamkepo E, Almesbahi AA, Naji M, Nasher SS, Rakesh A, Assiri AM, Sharma NC, Kariuki S, Pourshafie MR, Raugier J, Abubakar A, Carter JY, Wamala JF, Seguin C, Bouchier C, Malliavin T, Bakhshi B, Abulmaali HHN, Kumar D, Njoroge SM, Malik MR, Kiiru J, Luquero FJ, Azman AS, Ramamurthy T, Thomson NR, Quilici ML. 2019. Genomic insights into the 2016–2017 cholera epidemic in Yemen. *Nature* 565:230–233. <https://doi.org/10.1038/s41586-018-0818-3>.
 13. Ghosh P, Naha A, Pazhani GP, Ramamurthy T, Mukhopadhyay AK. 2014. Genetic traits of *Vibrio cholerae* O1 Haitian isolates that are absent in contemporary strains from Kolkata, India. *PLoS One* 9:e112973. <https://doi.org/10.1371/journal.pone.0112973>.
 14. Mutreja A, Kim DW, Thomson NR, Connor TR, Lee JH, Kariuki S, Croucher NJ, Choi SY, Harris SR, Lebens M, Niyogi SK, Kim EJ, Ramamurthy T, Chun J, Wood JL, Clemens JD, Czerkinsky C, Nair GB, Holmgren J, Parkhill J, Dougan G. 2011. Evidence for several waves of global transmission in the seventh cholera pandemic. *Nature* 477:462–465. <https://doi.org/10.1038/nature10392>.
 15. Imamura D, Morita M, Sekizuka T, Mizuno T, Takemura T, Yamashiro T, Chowdhury G, Pazhani GP, Mukhopadhyay AK, Ramamurthy T, Miyoshi S, Kuroda M, Shinoda S, Ohnishi M. 2017. Comparative genome analysis of VSP-II and SNPs reveals heterogenic variation in contemporary strains of *Vibrio cholerae* O1 isolated from cholera patients in Kolkata, India. *PLoS Negl Trop Dis* 11:e0005386. <https://doi.org/10.1371/journal.pntd.0005386>.
 16. Mekalanos JJ. 1983. Duplication and amplification of toxin genes in *Vibrio cholerae*. *Cell* 35:253–263. [https://doi.org/10.1016/0092-8674\(83\)90228-3](https://doi.org/10.1016/0092-8674(83)90228-3).
 17. Davis BM, Moyer KE, Boyd EF, Waldor MK. 2000. CTX prophages in classical biotype *Vibrio cholerae*: functional phage genes but dysfunctional phage genomes. *J Bacteriol* 182:6992–6998. <https://doi.org/10.1128/jb.182.24.6992-6998.2000>.
 18. Clark CA, Purins L, Kaewrakon P, Focareta T, Manning PA. 2000. The *Vibrio cholerae* O1 chromosomal integron. *Microbiology* 146:2605–2612. <https://doi.org/10.1099/00221287-146-10-2605>.
 19. Waldor MK, Rubin EJ, Pearson GD, Kimsey H, Mekalanos JJ. 1997. Regulation, replication, and integration functions of the *Vibrio cholerae* CTX Φ are encoded by region RS2. *Mol Microbiol* 24:917–926. <https://doi.org/10.1046/j.1365-2958.1997.3911758.x>.
 20. Moyer KE, Kimsey HH, Waldor MK. 2001. Evidence for a rolling-circle mechanism of phage DNA synthesis from both replicative and integrated forms of CTX Φ . *Mol Microbiol* 41:311–323. <https://doi.org/10.1046/j.1365-2958.2001.02517.x>.
 21. Kim EJ, Lee D, Moon SH, Lee CH, Kim DW. 2014. CTX prophages in *Vibrio cholerae* O1 strains. *J Microbiol Biotechnol* 24:725–731. <https://doi.org/10.4014/jmb.1403.03063>.
 22. Sarkar A, Morita D, Ghosh A, Chowdhury G, Mukhopadhyay AK, Okamoto K, Ramamurthy T. 2019. Altered integrative and conjugative elements (ICEs) in recent *Vibrio cholerae* O1 isolated from cholera cases, Kolkata, India. *Front Microbiol* 10:2072. <https://doi.org/10.3389/fmicb.2019.02072>.
 23. Pham TD, Nguyen TH, Iwashita H, Takemura T, Morita K, Yamashiro T. 2018. Comparative analyses of CTX prophage region of *Vibrio cholerae* seventh pandemic wave 1 strains isolated in Asia. *Microbiol Immunol* 62:635–650. <https://doi.org/10.1111/1348-0421.12648>.
 24. Ghosh P, Sinha R, Samanta P, Saha DR, Koley H, Dutta S, Okamoto K, Ghosh A, Ramamurthy T, Mukhopadhyay AK. 2019. Haitian variant *Vibrio cholerae* O1 strains manifest higher virulence in animal models. *Front Microbiol* 10:111. <https://doi.org/10.3389/fmicb.2019.00111>.
 25. Kim EJ, Yu HJ, Lee JH, Kim JO, Han SH, Yun CH, Chun J, Nair GB, Kim DW. 2017. Replication of *Vibrio cholerae* classical CTX phage. *Proc Natl Acad Sci U S A* 114:2343–2348. <https://doi.org/10.1073/pnas.1701335114>.
 26. Davis BM, Kimsey HH, Chang W, Waldor MK. 1999. The *Vibrio cholerae* O139 Calcutta bacteriophage CTX ϕ is infectious and encodes a novel repressor. *J Bacteriol* 181:6779–6787. <https://doi.org/10.1128/JB.181.21.6779-6787.1999>.
 27. Faruque SM, Tam VC, Chowdhury N, Diraphat P, Dziejman M, Heidelberg JF, Clemens JD, Mekalanos JJ, Nair GB. 2007. Genomic analysis of the Mozambique strain of *Vibrio cholerae* O1 reveals the origin of El Tor strains carrying classical CTX prophage. *Proc Natl Acad Sci U S A* 104:5151–5156. <https://doi.org/10.1073/pnas.0700365104>.
 28. Taylor RK, Miller VL, Furlong DB, Mekalanos JJ. 1987. Use of *phoA* gene fusions to identify a pilus colonization factor coordinately regulated with cholera toxin. *Proc Natl Acad Sci U S A* 84:2833–2837. <https://doi.org/10.1073/pnas.84.9.2833>.
 29. Naha A, Mandal RS, Samanta P, Saha RN, Shaw S, Ghosh A, Chatterjee NS, Dutta P, Okamoto K, Dutta S, Mukhopadhyay AK. 2020. Deciphering the possible role of *ctxB7* allele on higher production of cholera toxin by Haitian variant *Vibrio cholerae* O1. *PLoS Negl Trop Dis* 14:e0008128. <https://doi.org/10.1371/journal.pntd.0008128>.
 30. Samanta P, Ghosh P, Chowdhury G, Ramamurthy T, Mukhopadhyay AK. 2015. Sensitivity to polymyxin B in El Tor *Vibrio cholerae* O1 strain, Kolkata, India. *Emerg Infect Dis* 21:2100–2102. <https://doi.org/10.3201/eid2111.150762>.
 31. Samanta P, Mandal RS, Saha RN, Shaw S, Ghosh P, Dutta S, Ghosh A, Imamura D, Morita M, Ohnishi M, Ramamurthy T, Mukhopadhyay AK. 2020. A point mutation in *carR* is involved in the emergence of polymyxin B-sensitive *Vibrio cholerae* O1 El Tor biotype by influencing gene transcription. *Infect Immun* 88:e00080–20. <https://doi.org/10.1128/IAI.00080-20>.
 32. Zhang Y, Werling U, Edelmann W. 2012. SLICE: a novel bacterial cell extract-based DNA cloning method. *Nucleic Acids Res* 40:e55. <https://doi.org/10.1093/nar/gkr1288>.
 33. Wick RR, Judd LM, Gorrie CL, Holt KE. 2017a. Completing bacterial genome assemblies with multiplex MinION sequencing. *Microb Genom* 3:e000132. <https://doi.org/10.1099/mgen.0.000132>.
 34. Kolmogorov M, Yuan J, Lin Y, Pevzner PA. 2019. Assembly of long error-prone reads using repeat graphs. *Nat Biotechnol* 37:540–546. <https://doi.org/10.1038/s41587-019-0072-8>.
 35. Wick RR, Judd LM, Gorrie CL, Holt KE. 2017b. Unicycler: resolving bacterial genome assemblies from short and long sequencing reads. *PLoS Comput Biol* 13:e1005595. <https://doi.org/10.1371/journal.pcbi.1005595>.
 36. Walker BJ, Abeel T, Shea T, Priest M, Abouelliel A, Sakthikumar S, Cuomo CA, Zeng Q, Wortman J, Young SK, Earl AM. 2014. Pilon: an integrated tool for comprehensive microbial variant detection and genome assembly improvement. *PLoS One* 9:e112963. <https://doi.org/10.1371/journal.pone.0112963>.
 37. Faruque SM, Asadulghani Alim AR, Albert MJ, Islam KM, Mekalanos JJ. 1998b. Induction of the lysogenic phage encoding cholera toxin in naturally occurring strains of toxigenic *Vibrio cholerae* O1 and O139. *Infect Immun* 66:3752–3757. <https://doi.org/10.1128/IAI.66.8.3752-3757.1998>.
 38. Teppema JS, Guinée PA, Ibrahim AA, Pâques M, Ruitenberg EJ. 1987. In vivo adherence and colonization of *Vibrio cholerae* strains that differ in hemagglutinating activity and motility. *Infect Immun* 55:2093–2102. <https://doi.org/10.1128/IAI.55.9.2093-2102.1987>.
 39. Kaper JB, Bradford HB, Roberts NC, Falkow S. 1982. Molecular epidemiology of *Vibrio cholerae* in the U.S. Gulf Coast. *J Clin Microbiol* 16:129–134. <https://doi.org/10.1128/JCM.16.1.129-134.1982>.
 40. Hu D, Liu B, Feng L, Ding P, Guo X, Wang M, Cao B, Reeves PR, Wang L. 2016. Origins of the current seventh cholera pandemic. *Proc Natl Acad Sci U S A* 113:E7730–E7739. <https://doi.org/10.1073/pnas.1608732113>.
 41. Kaper JB, Nataro JP, Roberts NC, Siebeling RJ, Bradford HB. 1986. Molecular epidemiology of non-O1 *Vibrio cholerae* and *Vibrio mimicus* in the U.S. Gulf Coast region. *J Clin Microbiol* 23:652–654. <https://doi.org/10.1128/JCM.23.3.652-654.1986>.
 42. Lin W, Fullner KJ, Clayton R, Sexton JA, Rogers MB, Calia KE, Calderwood SB, Fraser C, Mekalanos JJ. 1999. Identification of a *Vibrio cholerae* RTX toxin gene cluster that is tightly linked to the cholera toxin prophage. *Proc Natl Acad Sci U S A* 96:1071–1076. <https://doi.org/10.1073/pnas.96.3.1071>.
 43. Octavia S, Salim A, Kurniawan J, Lam C, Leung Q, Ahsan S, Reeves PR, Nair GB, Lan R. 2013. Population structure and evolution of non-O1/non-O139 *Vibrio cholerae* by multilocus sequence typing. *PLoS One* 8:e65342. <https://doi.org/10.1371/journal.pone.0065342>.

44. Benítez JA, Silva AJ, Rodríguez BL, Fando R, Campos J, Robert A, García H, García L, Pérez JL, Oliva R, Torres CA, Ledón T. 1996. Genetic manipulation of *Vibrio cholerae* for vaccine development: construction of live attenuated El Tor candidate vaccine strains. *Arch Med Res* 27:275–283.
45. Waldor MK, Mekalanos JJ. 1994. Emergence of a new cholera pandemic: molecular analysis of virulence determinants in *Vibrio cholerae* O139 and development of a live vaccine prototype. *J Infect Dis* 170:278–283. <https://doi.org/10.1093/infdis/170.2.278>.
46. Allué-Guardia A, Echazarreta M, Koenig SSK, Klose KE, Eppinger M. 2018. Closed genome sequence of *Vibrio cholerae* O1 El Tor Inaba strain A1552. *Genome Announc* 6:e00098-18. <https://doi.org/10.1128/genomeA.00098-18>.
47. de Sá Morais LL, Garza DR, Loureiro EC, Nunes KN, Vellasco RS, da Silva CP, Nunes MR, Thompson CC, Vicente AC, Santos EC. 2012. Complete genome sequence of a sucrose-nonfermenting epidemic strain of *Vibrio cholerae* O1 from Brazil. *J Bacteriol* 194:2772. <https://doi.org/10.1128/JB.00300-12>.
48. Yamamoto S, Lee K, Morita M, Arakawa E, Izumiya H, Ohnishi M. 2018. Single circular chromosome identified from the genome sequence of the *Vibrio cholerae* O1 bv. El Tor Ogawa strain V060002. *Genome Announc* 6:e00564-18. <https://doi.org/10.1128/genomeA.00564-18>.
49. Pang B, Yan M, Cui Z, Ye X, Diao B, Ren Y, Gao S, Zhang L, Kan B. 2007. Genetic diversity of toxigenic and nontoxigenic *Vibrio cholerae* serogroups O1 and O139 revealed by array-based comparative genomic hybridization. *J Bacteriol* 189:4837–4849. <https://doi.org/10.1128/JB.01959-06>.
50. Bourgeois J, Lazinski DW, Camilli A. 2020. Identification of spacer and protospacer sequence requirements in the *Vibrio cholerae* type I-E CRISPR/Cas system. *mSphere* 5:e00813-20. <https://doi.org/10.1128/mSphere.00813-20>.
51. Bernardy EE, Turnsek MA, Wilson SK, Tarr CL, Hammer BK. 2016. Diversity of clinical and environmental isolates of *Vibrio cholerae* in natural transformation and contact-dependent bacterial killing indicative of type VI secretion system activity. *Appl Environ Microbiol* 82:2833–2842. <https://doi.org/10.1128/AEM.00351-16>.
52. Okada K, Roobthaisong A, Swaddiwudhipong W, Hamada S, Chantaroj S. 2013. *Vibrio cholerae* O1 isolate with novel genetic background, Thailand-Myanmar. *Emerg Infect Dis* 19:1015–1017. <https://doi.org/10.3201/eid1906.120345>.
53. Reimer AR, Van Domselaar G, Stroika S, Walker M, Kent H, Tarr C, Talkington D, Rowe L, Olsen-Rasmussen M, Frace M, Sammons S, Dahourou GA, Boncy J, Smith AM, Mabon P, Petkau A, Graham M, Gilmour MW, Gerner-Smidt P, *V. cholerae* Outbreak Genomics Task Force. 2011. Comparative genomics of *Vibrio cholerae* from Haiti, Asia, and Africa. *Emerg Infect Dis* 17:2113–2121. <https://doi.org/10.3201/eid1711.110794>.
54. Fu Y, Ho BT, Mekalanos JJ. 2018. Tracking *Vibrio cholerae* cell-cell interactions during infection reveals bacterial population dynamics within intestinal microenvironments. *Cell Host Microbe* 23:274–281. <https://doi.org/10.1016/j.chom.2017.12.006>.
55. Okada K, Natakathung W, Na-Ubol M, Roobthaisong A, Wongboot W, Maruyama F, Nakagawa I, Chantaroj S, Hamada S. 2015. Characterization of 3 megabase-sized circular replicons from *Vibrio cholerae*. *Emerg Infect Dis* 21:1262–1263. <https://doi.org/10.3201/eid2107.141055>.
56. Stutzmann S, Blokesch M. 2016. Circulation of a quorum-sensing-impaired variant of *Vibrio cholerae* strain C6706 masks important phenotypes. *mSphere* 1:e00098-16. <https://doi.org/10.1128/mSphere.00098-16>.
57. Folster JP, Katz L, McCullough A, Parsons MB, Knipe K, Sammons SA, Boncy J, Tarr CL, Whichard JM. 2014. Multidrug-resistant IncA/C plasmid in *Vibrio cholerae* from Haiti. *Emerg Infect Dis* 20:1951–1953. <https://doi.org/10.3201/eid2011.140889>.
58. Reyes-Robles T, Dillard RS, Cairns LS, Silva-Valenzuela CA, Housman M, Ali A, Wright ER, Camilli A. 2018. *Vibrio cholerae* outer membrane vesicles inhibit bacteriophage infection. *J Bacteriol* 200:e00792-17. <https://doi.org/10.1128/JB.00792-17>.
59. Irengue LM, Durant JF, Ambroise J, Mitangala PN, Bearzatto B, Gala JL. 2020. Genome sequence of a pathogenic *Vibrio cholerae* O1 El Tor strain defective for the entire *Vibrio* pathogenicity island 1, isolated in eastern Democratic Republic of the Congo. *Microbiol Resour Announc* 9:e00454-20. <https://doi.org/10.1128/MRA.00454-20>.
60. Overmars L, van Hijum SAFT, Siezen RJ, Francke C. 2015. CiVi: circular genome visualization with unique features to analyze sequence elements. *Bioinformatics* 31:2867–2869. <https://doi.org/10.1093/bioinformatics/btv249>.